Construction and Building Materials 213 (2019) 306–312

Contents lists available at ScienceDirect

Construction and Building Materials

journal homepage: www.elsevier.com/locate/conbuildmat

The utilization of sulfite-rich Spray Dryer Absorber Material in portland cement concrete

Naser P. Sharifi [a,*], Robert B. Jewell [b], Tristana Duvallet [b], Anne Oberlink [b], Tom Robl [b], Kamyar C. Mahboub [a], Ken J. Ladwig [c]

[a] Department of Civil Engineering, University of Kentucky, Lexington, KY 40506, USA
[b] Center for Applied Energy Research, University of Kentucky, Lexington, KY 40511, USA
[c] Electric Power Research Institute, 3420 Hillview Avenue, Palo Alto, CA 94304, USA

HIGHLIGHTS

- Utilization potential of Spray Dryer Absorber Material (SDAM) as an additive in concrete was determined.
- A 20 wt% replacement of OPC with SDAM yielded a concrete that met the desirable 28-day performance criteria.
- The results provide evidence against the stigma of poor durability when using SDAM in concrete.

ARTICLE INFO

Article history:
Received 12 October 2018
Received in revised form 28 March 2019
Accepted 8 April 2019

Keywords:
Spray Dryer Absorber Material
Dry scrubber ash
OPC replacement
Concrete performance
Coal combustion byproducts

ABSTRACT

The objective of this study was to determine the utilization potential of Spray Dryer Absorber Material (SDAM) as an additive in concrete made with portland cement. Utilizing SDAM for beneficial use such as portland cement replacement reduces the CO_2 impact for every cubic meter of concrete placed, and provides a means for utilities to avoid the impacts of landfilling. The utilization of SDAM in concrete is often avoided due to delay in setting time, i.e. early-age strength-gain, and expansion related durability issues. The study included SDAM collected from five different coal combustion utilities. A series of laboratory experiments were conducted on the fresh and hardened concrete made by replacing 20 wt% of the portland cement. The findings of this research demonstrates that despite slow strength gain at early ages, a 20 wt% replacement of portland cement yielded a concrete that met the desirable 28-day performance criteria. Additionally, the incorporation of SDAM containing elevated levels of fly ash content improved the resistance to chloride permeability, and autoclave expansion resistance of concrete. These results provide evidence against the stigma of poor durability when using SDAM in concrete.

1. Introduction

Coal-fired power plants are subject to regulations that require control of sulfur dioxide emissions and other acid gases [1]. Installation of Flue Gas Desulfurization (FGD) systems in the coal-fired power plants is considered an effective strategy to reduce the sulfur dioxide emission. This technology gained prominence in the 1980s, and since then, a variety of FGD systems have been used all around the world [1]. As of 2007 in the U.S., about 85% of FGD systems are wet, and 3% are dry injection systems. The remaining 12% of FGD systems are Spray Dryer Absorber (SDA) systems [2].

The SDA systems, or semidry systems, used for FGD come in a variety of configurations. The process used in SDA systems consists of four operations: sorbent preparation, the spray dryer absorber, particulate collection, and byproduct handling systems [2,3]. Depending on the collection and process flow, different types of solids are collected. The SDA Material (SDAM) is generally a mix of fly ash and calcium-sulfur compounds. SDAM can range from materials essentially devoid of fly ash to one that is a mix of predominantly fly ash. SDAM differs from more traditional wet forced oxidation FGD gypsum, in that it contains primarily calcium sulfite instead of calcium sulfate, with calcium hydroxide and minor amounts of calcium carbonate.

An alkaline sorbent (primarily calcium oxide, CaO pre-calcined) is mixed with water. The aqueous slurry is sprayed into the hot flue gas in the spray dryer absorber through an atomizer that produces a dense cloud of small droplets. When the atomized lime slurry is

* Corresponding author.
E-mail address: npsharifi@uky.edu (N.P. Sharifi).

https://doi.org/10.1016/j.conbuildmat.2019.04.074
0950-0618/

introduced to the hot flue gas, SO_2, SO_3, and Cl quickly react with the sorbent while the water evaporates. A fly ash pre-collection system, such as an Electrostatic Precipitator (ESP), is often used prior to the SDA. However, there are many cases where there is no ESP and the fly ash is captured as part of the SDAM. The efficiency of the fly ash pre-collection system will determine the volume of fly ash that is captured with the SDAM. The reacted material from the SDA is a dry powder byproduct, comprised primarily of calcium sulfite ($CaSO_3$), which hydrates to the mineral hannebachite ($CaSO_3{\cdot}H_2O$). Some of the dry byproduct is collected from the bottom of the absorber; however, the bulk of the SDA material is collected in either a fabric filter/baghouse or an ESP.

Most of the SDAM is landfilled. The American Coal Ash Association (ACAA) production and use survey reports 21% of the 1.5 million tons of dry FGD produced was utilized primarily for mining applications and waste stabilization/solidification in 2016 [4]. The low SDAM utilization rate emphasizes the need for research to identify promising high-volume applications for this material. This need was the driver for studying the influence of SDAM in OPC concrete.

The morphology and chemistry of SDAM, particularly those with elevated amounts of fly ash, allow them to contribute to the performance and durability of portland cement concrete [5]. OPC is one of the most widely used construction materials in the world [6]. The production of OPC is a very energy intense process with a high environmental footprint through CO_2 emissions [7]. Therefore, utilizing SDAM as a partial replacement for OPC could lead to a lower energy, lower CO_2 concrete product [8]. Additionally, depending on the mineralogy and morphology of the SDAM, this replacement improves some of the key properties of concrete. However, there is little publically available information on the use of SDAM in concrete and other cementitious products. Low quantities of produced SDAMs, less than 0.5%, are utilized by the concrete industry [2,4]. The low utilization rate in the concrete industry is partially related to low early-age compressive strength and potential for expansion [9,10]. However, research results show this is not always the case and is highly dependent on the conditions in which the SDAM was produced.

Therefore, the primary objective of this research was to study the application of SDAM in concrete as a partial replacement for OPC, and evaluate the issues that prevent utilization of this material in the concrete industry. SDAMs were acquired from five separate coal combustion power plants. The samples were then characterized by analyzing the chemical, mineralogical, and physical properties. Five concrete mixes were proportioned, by replacing 20 wt% of OPC with SDAM. A series of laboratory experiments were conducted to evaluate the hydration effects of an OPC/SDAM blend on the fresh and hardened concrete properties. MINITAB software was used to apply the ANOVA and Tukey's test for pairwise comparisons to provide a statistical interpretation of the experimental results.

2. Materials and methods

2.1. Materials

2.1.1. Cement, aggregates, and additives

A Type I Ordinary Portland Cement (OPC) with specific gravity of 3.15 g/cm^3 and meeting ASTM C150 requirements was used in each concrete batch. Aggregates were received in bulk, and consisted of a 20 mm coarse crushed limestone aggregate, a 10 mm intermediate crushed limestone aggregate, and a river sand. Aggregate specific gravities were 2.68, 2.71, and 2.62 g/cm^3, respectively. Results for the particle size analysis of the aggregates are shown in Fig. 1. In addition, comparisons between the passing percentages of each sieve and the ASTM C33 requirements are presented in Table 1.

An air entrainer was used to attain the desired 6% entrained air in the concrete mixes. The air entrainer incorporates tiny bubbles which relieve internal pressure on the concrete by allowing small pockets of space for water to expand when it freezes. Additionally, a water reducer, Glenium 3030, was added to the mix to help reduce the amount of required mixing water, while maintaining a constant consistency, i.e. slump.

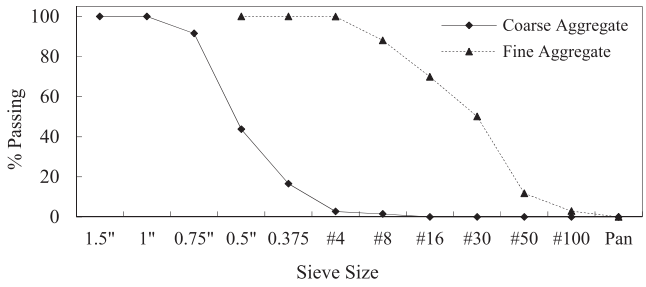

Fig. 1. Particle size analysis of the aggregate.

2.1.2. Spray Dryer Absorber Material (SDAM)

In this study, five different SDAMs were acquired from coal-fired power companies. The chemical composition of the SDAMs, designated M1 to M5, is presented in Table 2. The SDAMs can be divided into two groups: Group 1 – M1, M3, and M4 with high percentages of CaO and SO_3 and low percentages of SiO_2 and Al_2O_3; Group 2 – M2, and M5 with low CaO and SO_3 and high SiO_2 and Al_2O_3. The higher SiO_2 and Al_2O_3 contents imply that M2 and M5 contain higher amounts of fly ash. The chemical composition of a fly ash-rich SDAM evaluated in a previous EPRI funded study revealed that the weight percentage of SiO_2 was in the range of 38% to 46%, and the weight percentage of Al_2O_3 was in the range of 17% to 21%; which matches the measured chemical composition of M2 and M5 [11,12].

2.1.2.1. Particle size distribution. The particle size distribution of all materials were measured using a Malvern Mastersizer 2000 laser particle-size analyzer. The measurements were conducted in isopropanol to avoid hydration of the samples. The particle size distribution of SDAM is important as it affects many engineering parameters, such as chemical reactivity [2]. The results of the particle size distribution are presented in Table 3, and Fig. 2. The results show that among all the SDAMs, M2 and M5 are comprised of larger particles. This is attributed to the higher fly ash content in these SDAMs.

2.1.2.2. Normal consistency. Normal consistency of the SDAMs was measured using a Vicat apparatus based on the ASTM C187 standard. This test measures the quantity of water required to form a uniform paste. The results for the normal consistency of OPC and the SDAMs are presented in Table 3. Among all SDAMs, M2 and M5 exhibited relatively lower normal constituency. This means that compared to M1, M3, and M4, the M2 and M5 SDAMs require a lower water content to reach a similar flow-ability. This is attributed to the relatively larger particle sizes of M2 and M5. Similar to the previous set of results, this may be attributed to higher fly ash content in these SDAMs.

2.1.2.3. X-ray diffraction. X-ray diffraction (XRD) analyses were performed on the SDAMs with a Philips X'Pert diffractometer (model PW3040-PRO) operating at 45 kV and 40 mA and utilizing Cu K-alpha radiation. The samples were ground by hand in a ceramic mortar and pestle, and dry mounted in aluminum holders. The step size for the analysis was 0.017 degrees at 0.035 degrees/second over 8–60 degrees 2-tehta. The crystalline phases were identified with an International Centre for Diffraction DATA (ICDD) powder diffraction (PDF) database. The XRD results for OPC and each SDAM are summarized in Table 4. The results show that portlandite and hannebachite are the only two mineral phases that are present in all the SDAMs. Based on a study on fifty-nine SDAM products, portlandite and hannebachite were the phases that all the combustion products contained [13]. It was reported that portlandite resulted from using an excess amount of sorbent. Hannebachite was the primary product of sorbent reaction with SO_2 in the flue gas [13]. The abundance of quartz in M2 and M5 is the result of high fly ash content in these two SDAMs.

2.1.2.4. Scanning electron microscopy. A scanning electron microscope (SEM) was used to analyze the morphology of the particles of each material, as well as the concrete samples after 15 months of curing. Samples for SEM analyses were analyzed on as-received SDAM samples, and on broken fragments from the inside of the concrete samples. The concrete fragments had to be immersed in isopropanol for a couple of days to halt the hydration process and remove the water. Following this step, the fragments were dried in an oven at 45 °C until dry. The as-received samples were placed directly on a carbon tape, while the dried concrete fragments were placed on a carbon tape with additional carbon paint for better adhesion and conductivity of the surface of the samples. After placing the samples on a carbon tab, the specimens were coated with gold, and the SEM analyses were performed on a Hitachi S-4800 operating at a voltage of 5 kV and a current of 10 micro-amperes.

Table 1
Comparison between the particle size analysis of the aggregates and the ASTM C33 requirements.

Coarse Aggregate				Fine Aggregate			
Sieve Size	% Passing	% Passing Requirement	Result	Sieve Size	% Passing	% Passing Requirement	Result
1.5″	100.00	100	Pass	0.375	100.00	100	Pass
1″	100.00	95–100	Pass	# 4	99.90	95–100	Pass
0.75″	91.55	–	–	# 8	88.05	80–100	Pass
0.5″	43.77	25–60	Pass	# 16	69.88	50–85	Pass
0.375	16.58	—	—	# 30	50.10	25–60	Pass
#4	2.70	0–10	Pass	# 50	11.76	5–30	Pass
#8	1.48	0–5	Pass	# 100	2.91	0–10	Pass
Pan	0.00	–	–	Pan	0.00	–	–

Table 2
Chemical compositions of OPC and the SDAMs in weight percentages.

Material	CaO	SO_3	SiO_2	Al_2O_3	Fe_2O_3	MgO	Na_2O	K_2O	P_2O_5	SrO	BaO	TiO_2
OPC	61.95	2.96	21.89	6.23	2.53	2.85	0.11	0.71	0.1	NA*	NA*	0.26
M1	***51.12***	***32.08***	7.35	4.35	1.29	2.08	0.66	0.20	0.27	0.12	0.19	0.28
M2	28.07	7.18	***34.8***	***17.41***	5.12	3.34	1.07	0.45	0.67	0.25	0.44	1.16
M3	***48.41***	***45.32***	2.19	1.47	0.44	1.62	0.19	0.06	0.13	0.05	0.06	0.03
M4	***52.33***	***43.71***	1.49	0.78	0.34	1.02	0.08	0.07	0.08	0.03	0.03	0.00
M5	26.6	11.35	***29.75***	***17.03***	5.16	3.81	2.79	0.58	0.88	0.29	0.50	1.21

*Not available.

Table 3
Physical properties of OPC and the SDAMs.

Material	Particle size analysis in μm			Normal Consistency (%)	Density (kg/m^3)
	d (10)	d (50)	d (90)		
OPC	2.55	16.85	47.89	25.4	3150
M1	1.0	4.0	62.3	30.8	2427
M2	1.7	***30.7***	164.0	***23.9***	2523
M3	0.9	3.0	20.0	29.3	2439
M4	1.0	3.9	125.7	29.2	2479
M5	2.0	***17.5***	51.6	***25.3***	2599

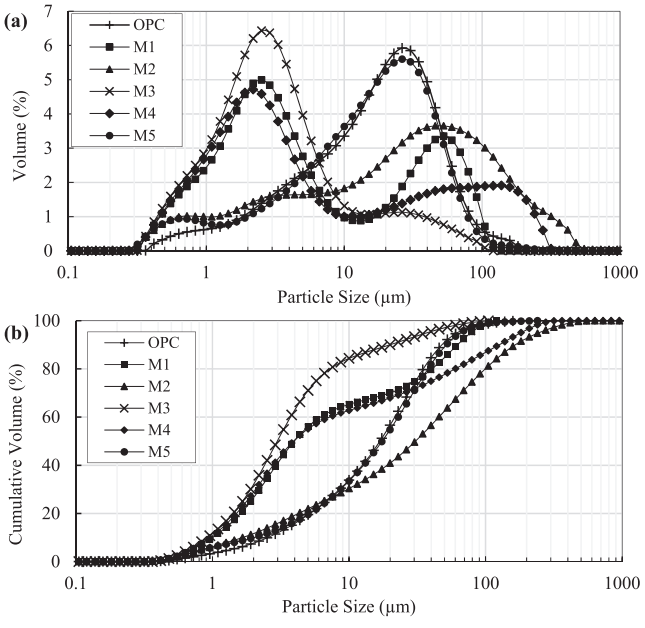

Fig. 2. Particle size distribution of OPC the SDAMs. a) Volume percentage of the particle sizes. b) Cumulative volume percentage of the particle sizes.

The results of the SEM analysis for the SDAM samples are presented in Fig. 3, and for the hardened concrete mixtures containing the SDAMs are presented in Fig. 4. Some of the hydration products are specified in the images. SEM images presented in references [14–17] were used to identify the specified phases. The formation of C-S-H and Portlandite is consistent with the present of 80 wt% OPC in the mixture. In addition, the ettringite formation is consistent with the presence of tricalcium aluminate from OPC, which hydrates to ettringite with the presence of calcium sulfate (Fig. 4).

The results of chemical composition, normal consistency, XRD, and SEM experiments show that among all the SDAMs, the M2 and M5 sources contain a higher amount of fly ash. Later in this study, it will be explained how this property and other characteristics of the SDAMs, will affect different chemical, physical, and mechanical properties of the concrete that they are used in.

2.2. Methods

2.2.1. Mix design and maximum SDAM percentage

Six different mixes were prepared. In Mix S0, the control mix, no SDAM was incorporated. In mixes S1, S2, S3, S4, and S5, 20 wt% of OPC was replaced with M1, M2, M3, M4, and M5, respectively. Based on previous research, 20 wt% replacement of OPC with SDAM was sufficient to achieve a performance threshold similar to that of concrete with no SDAM, without greatly affecting the setting time [5]. Additionally, in similar studies that evaluated the effect of SDAM incorporation in concrete's performance, 20 wt% of cement was replaced by SDAM [18,19]. The concrete mixes targeted a 0.49 water to cement ratio with a 28-day compressive strength of 28 MPa. Details of the mix proportioning of all the mixes are provided in Table 5.

2.2.2. Fresh concrete properties

2.2.2.1. Slump. ASTM C143 procedures were followed to determine the slump, or workability, of each prepared concrete mix. Generally, slump is targeted between 9.0 cm and 12.0 cm. In this study, the slump was allowed to be outside of the normal parameters due to the additional, uncharacteristic materials used in the formulations. The results for the slump test of all mixes are presented in Table 6.

2.2.2.2. Air content. Air content was measured using a pressure Type B meter, according to ASTM C231. The air content target for each mix was 4.5%, which would provide acceptable protection from freeze-thaw. The results for the air content of all mixes are presented in Table 6.

Table 4
Detection of mineral phases in OPC and SDAMs. (Tr. = Traces, X = Mineral phase present, XXX = Mineral phase abundant).

Minerals		Material					
Name	Cement Notation	OPC	M1	M2	M3	M4	M5
Anhydrite	$C\bar{S}$	Tr.	–	–	–	X	–
Bassanite or Hemihydrate	$C\bar{S}H_{1/2}$	–	–	–	–	–	X
Belite	C_2S	X	–	–	–	–	–
Brownmillerite	C_4AF	X	–	–	–	–	–
Calcite	$C\dot{C}$	–	X	–	Tr.	XXX	XXX
Calcium Aluminum Oxide Hydrate	C_2AH_8	–	–	Tr.	–	–	–
Ettringite	$C_6AS_3H_{32}$	–	–	Tr.	–	–	X
Gehlenite	C_2AS	–	–	Tr.	–	–	–
Gypsum	$C\bar{S}H_2$	–	–	–	–	XXX	XXX
Hannebachite	$CaSO_30\cdot.5H_2O$	–	X	X	XXX	XXX	X
Hatrurite (or Alite)	C_3S	XXX	–	–	–	–	–
Periclase	M	X	–	Tr.	–	–	X
Portlandite	CH	–	XXX	XXX	XXX	X	Tr.
Quartz	S	–	Tr.	XXX	–	–	XXX
Tricalcium Aluminate	C_3A	X	–	Tr.	–	–	–

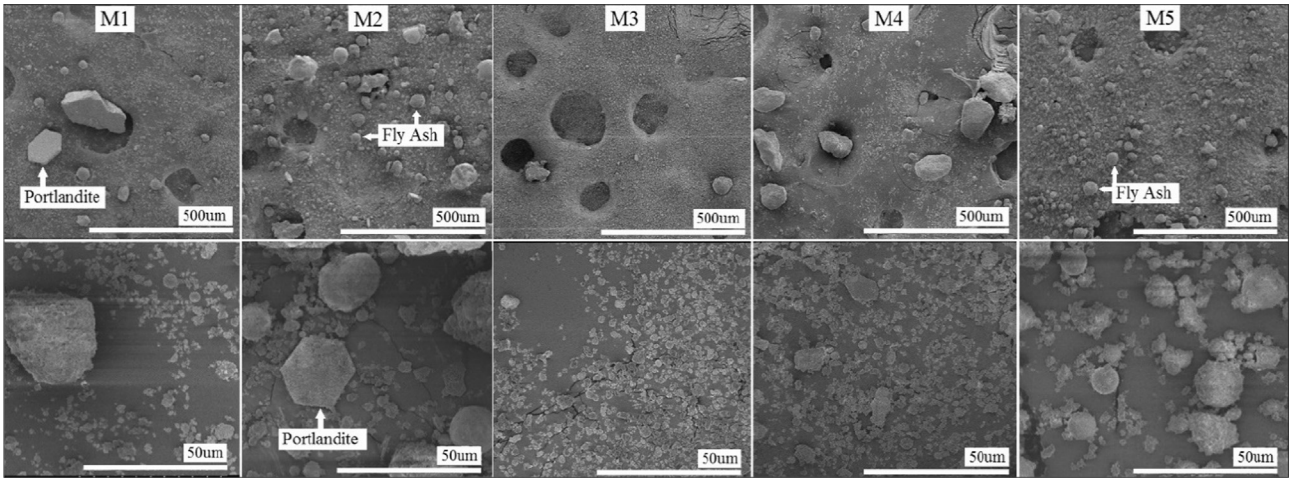

Fig. 3. SEM images of the five SDAMs. The magnification of the pictures in the first row is 100X, and the magnification of the pictures in the second row is 1000X.

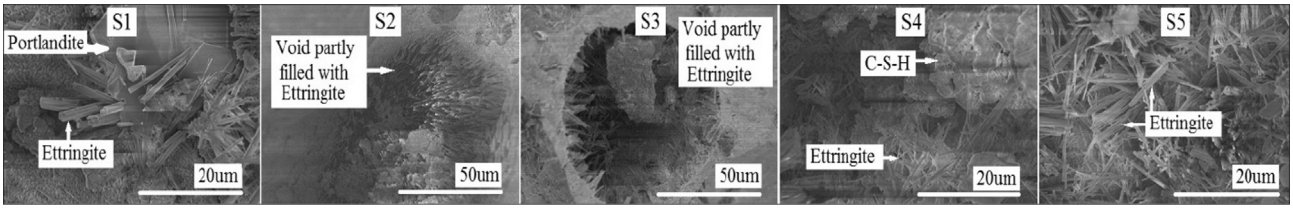

Fig. 4. SEM images concrete mixtures containing five SDAMs.

Table 5
Mix proportioning of the six mixes.

Mix	OPC (kg/m^3)	SDAM (kg/m^3)	Coarse Agg.* (kg/m^3)	Intermediate Agg. (kg/m^3)	Fine Agg. (kg/m^3)	Water (kg/m^3)	Water Reducer (ml/m^3)	AEA** (ml/m^3)
S0	307.0	00.0	630.9	374.7	834.0	149.9	0.69	0.31
S1	245.6	61.4	625.6	371.5	827.0	149.6	0.69	0.31
S2	245.6	61.4	626.6	372.1	828.3	150.1	0.00	0.31
S3	254.6	61.4	625.4	371.4	826.7	149.6	0.69	0.31
S4	254.6	61.4	626.2	371.9	827.7	149.8	0.37	0.31
S5	254.6	61.4	627.0	372.4	828.8	149.8	0.37	0.31

* Aggregate.
** Air Entraining Admixture.

Table 6
Fresh concrete properties.

Mix	w/c*	Slump (cm)	Air Content (%)
S0	0.49	7.6	3.2
S1	0.49	9.4	7.0
S2	0.49	15.0	7.0
S3	0.47	15.1	6.8
S4	0.47	10.1	6.5
S5	0.47	14.5	7.5

* Water:cement ratio.

2.2.3. Hardened concrete properties

2.2.3.1. Compressive strength. ASTM C39 procedures were followed for the compressive strength test. After mixing, the concrete mixture was placed in 7.62 cm × 15.24 cm plastic cylindrical molds. The molds then were capped for 24 h, and after demolding, the specimens were kept in a curing room with constant temperature and humidity. For each mix formulation, 18 specimens were prepared, with three specimens tested at 1, 7, 14, 28, 56, and 112 days. Before the test, each specimen was capped with sulfur compound in accordance with ASTM C617 to ensure that the test cylinder had smooth, parallel, and uniform bearing surfaces that were perpendicular to the applied axial load during the test. The loading rate was 15 MPa/min for all compressive strength specimens.

2.2.3.2. Flexural strength. ASTM C78 procedures were followed for the flexural strength test. After mixing, the concrete mixture was placed in 7.62 cm × 7.62 cm × 30.48 cm stainless steel prism molds. The molds were covered for 24 h. After demolding, the specimens were kept in a curing chamber. For each mix formulation, 12 specimens were prepared, with two specimens tested at 1, 7, 14, 28, 56, and 112 days. The loading rate was 1 MPa/min for all beam specimens.

2.2.4. Concrete durability

2.2.4.1. Surface resistivity. Rapid Chloride Permeability (RCP) is a widely used method to assess concrete durability. However, this test is labor intensive. Alternatively, a Surface Resistivity (SR) test, a nondestructive test, was conducted on the cylindrical specimens before testing them for compressive strength. In the SR test, the ability of the concrete to conduct electrical current is measured using a Wenner 4-probe array. Various studies have shown a good correlation between RCP and SR data [20–22]. Surface resistivity of each specimen was measured using the Resipod Proceq device, with a probe spacing of 3.8 cm. For each specimen, the resistivity was measured at four different locations around the circumference of the cylinder, and the average was recorded as the surface resistivity of the specimen.

2.2.4.2. Autoclave expansion. Autoclave expansion test was conducted on OPC and SDAM cement paste samples following ASTM C151. The first paste sample, AE0, only contained portland cement. However, in the other five paste samples, distinguished as AE1 to AE5, 20 wt% of OPC was replaced with M1 to M5 SDAMs, respectively. This test provides information on potential delayed expansion that may be caused by the hydration of calcium oxide (CaO), or periclase (MgO), or both, when present in cement or SDAMs. Beforehand, the consistency for each composition was determined by following ASTM C187. When the normal consistency was identified, two autoclave bars for each composition were prepared in molds and cured in a moist closet for 24 h before removing them from the molds. The samples were then placed in an autoclave maintained at a pressure of 2 MPa for 3 h. The change in length of the cement specimens was calculated by subtracting the length of the samples before from that after the experiment, and reported as percent of the effective gage length. As indicated in the ASTM C151, a minus sign prefixed to the percent value indicates a decrease in length, while a positive sign indicates an increase in length.

3. Results and discussion

3.1. Concrete performance testing

3.1.1. Compressive strength

Results of the compressive strength test are presented in Fig. 5. MINITAB software was used to conduct Analysis of Variance (ANOVA) as well as Tukey's test for pairwise comparisons in order to statistically study the compressive strength data. At the significance level of alpha = 0.05 (or confidence level of 95%), there is evidence to conclude that at all ages the mean compressive strength of all the mixes that contained SDAMs differed significantly from the control mix. This drop in the compressive strength was between 10% and 20% for the SDAM samples. Also, based on the statistical analysis for the samples at the age of 28 days, mixes S1 to S4 fall in the same category, and they all reach the desired compressive strength. However, the compressive strength of S5 is significantly less than the other mixes, and it does not reach to the required 28-day compressive strength. After 112 days of curing, the S5 also reached to the desired compressive strength.

At the age of 7 days, the results of the statistical analysis showed that the compressive strengths of S1, S2, and S3 were significantly different from S4 and S5. As the results of the XRD show in Table 4, M1, M2, and M3 have higher amounts of portlandite compared to M4 and M5. Crystallization of portlandite increases the content of cement hydration products, and leads to increase in the compressive strength of concrete [23]. Therefore, higher compressive strengths of S1, S2, and S3 at 7-days may be attributed to the higher portlandite content in M1, M2, and M3.

These results suggest that the sufficiency of compressive strength at the age of 7 days depends on the specific construction requirement; however, all the mixes that contain SDAM, except M5, pass the compressive strength requirement for pavement application (AASHTO T 97).

The results also show that there is an increase in the compressive strength for all the mixes after the age of 28 days. The difference between the compressive strength of the mixes that contained SDAM and the control mix decreased as the age of curing increased. This increase in the compressive strength at higher ages may be attributed to the pozzolanic reaction of fly ash. As it has been reported in previous studies, the compressive strength of a concrete containing fly ash could continuously increase for up to 720 days [24].

3.1.2. Flexural strength

The results of the flexural strength test are presented in Fig. 6. The statistical analysis showed that at the age of 1-day, the flexural strength of all the mixes that contained SDAMs was significantly lower than the flexural strength of the control mix. However, at the age of 7-days, the flexural strength of all the mixes that contained SDAM, except S4, was statistically equal to the control mix. At the age of 28-days, the flexural strength of S1, S4, and S5 fall in the same category as S0, but the flexural strength of S2 and S3 were significantly higher that the control mix. Also, at the ages of 56-days and 112-days, the flexural strength of all the SDAM samples was significantly higher that the control mix. The particular trend of compressive and flexural strengths not increasing in the same direction appears to be an anomaly and counterintuitive. More research is needed to address this issue.

3.2. Concrete durability

3.2.1. Surface resistivity

The results of the surface resistivity test are presented in Fig. 7. Based on the statistical analysis, at a significance level of 0.05, there is evidence to conclude that for day 1, the mean surface resistivity of all the mixes that contained SDAM was significantly less than the control mix. However, at day-7, there was not significant difference between Mixes S2, S5, and Mix S0. At 28 days of curing, S1, S3, and S4 had similar surface resistivity as the control mix. Based on the categorization presented by Chini et al., because the 28-day surface resistivity of all the mixes fall between 12 kΩ and 21 kΩ, they all have moderate chloride ion permeability [21]. However, at 56 and 112 days of curing, the surface resistivity of S2 and S5 were higher by 38% and 57% as compared to the control mix (S0). The increased resistivity is attributed to the higher fly ash content in M2 and M5. Researchers have shown that the incorporation of fly ash significantly increases the resistance to chloride ion permeability of concrete [19,25].

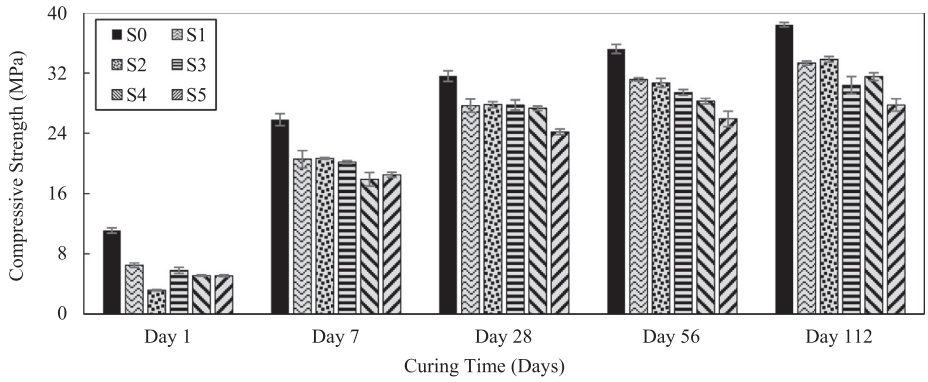

Fig. 5. Compressive strength of the six mixes at different ages.

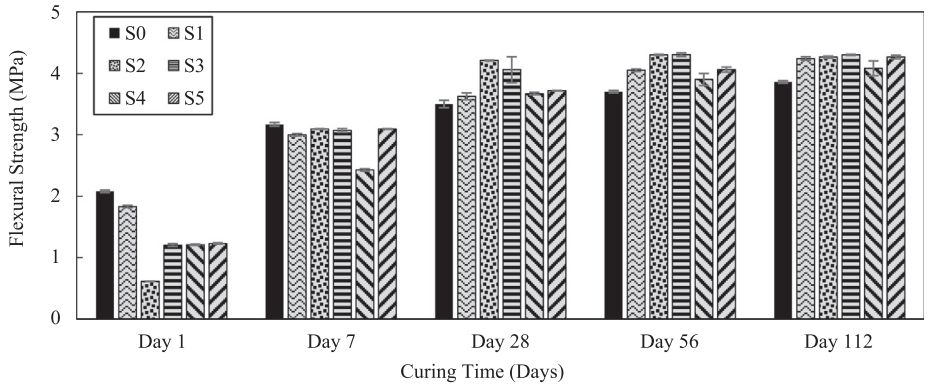

Fig. 6. Flexural strength of the six mixes at different ages.

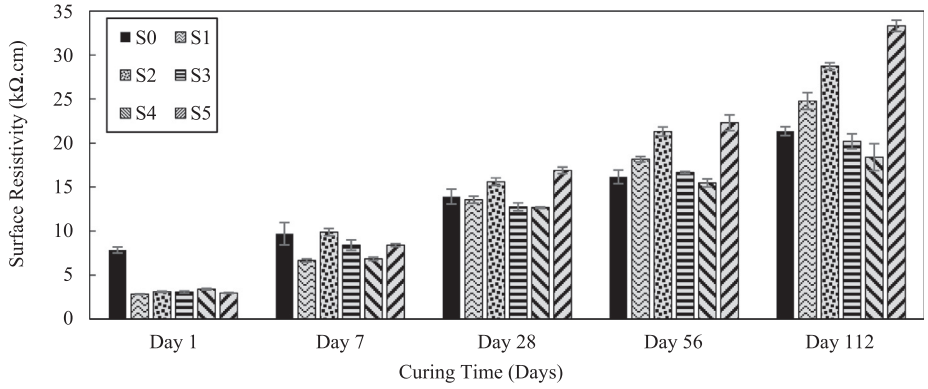

Fig. 7. Surface resistivity of the SDAM concrete.

An increase in surface resistivity translates to an increase in resistance against chloride attack. Therefore, compared to OPC concrete, a concrete that contains M2 and M5 SDAMs would have a more reliable performance in locations with harsh chloride conditions. This is consistent with the results presented in [12], where it was reported that incorporation of SDAMs in concrete yields durability performance comparable to or superior to the reference concrete. For applications such as bridge decks, piles, seawalls, shoreline stabilization, where the concrete structure is exposed to chloride attack, it is expected that the utilization of M2 and M5 SDAMs increases the service life of the concrete structure.

3.2.2. Autoclave expansion

As described in ASTM C618, the maximum autoclave expansion or contraction limit is set at 0.8%. The results of the autoclave test are presented in Fig. 8. The autoclave expansion of all the paste samples were less than 0.05%, which is well below the maximum limit set by ASTM C618.

Considering all paste samples, AE2 and AE5, which contained M2 and M5 SDAMs, had the lowest autoclave expansion. The higher fly ash content in M2 and M5 leads to elevated levels of Al_2O_3 content. Based on a previous research, the incorporation of a relatively high volume of fly ash in concrete mix controlled the expansion of concrete, even for the cases that highly reactive

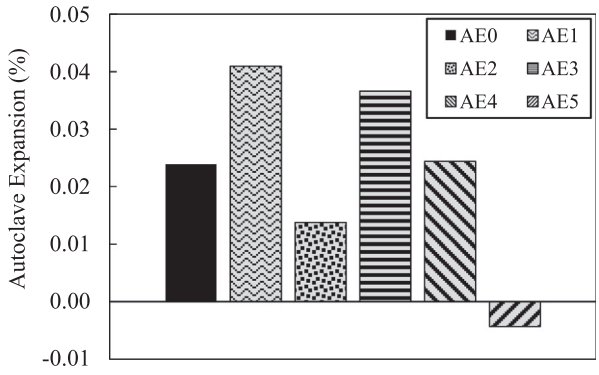

Fig. 8. Autoclave expansion percentage of the six mixes.

aggregates were used in the concrete [12], which are consistent with the results presented in [25]. These results suggest that the incorporation of SDAMs with elevated fly ash content in concrete could protect the concrete against the expansion caused by different chemical reactions at higher ages of concrete.

4. Conclusion and future work

This study investigated the potential use of SDAMs as partial replacements for OPC in concrete. Utilizing SDAMs for beneficial use, such as OPC replacement, contributes to reducing the impact on increasing volumes of these useful scrubber materials being landfilled. Partial replacement (20 wt% of cement) of OPC with SDAM in concrete provides benefit by decreasing cost and improving chloride penetration resistance, and resistance to autoclave expansion, while exhibiting compressive strength performance similar to that of a concrete with 100% Type-I Portland cement. Despite slow strength-gain at early ages, a 20 wt% replacement of OPC yielded a concrete that met performance criteria by 28 days of curing. Research is currently underway to enhance the early-age strength gain of concrete containing spray dryer ash material. In addition, conducting ASR and Drying Shrinkage tests to better understand the effects of incorporation of SDAMs on the durability of concrete is suggested as future work.

Conflict of interest

The authors declare no conflict of interest.

Acknowledgements

The authors gratefully acknowledge financial support for this research through a grant funded by the Electric Power Research Institute (EPRI).

References

[1] T.D. Berland et al., Review of Handling and Use of FGD Material; CARRC Final Report for Utility Solid Waste Activities Group, EERC Publication No. 2003-EERC-04-04; Grand Forks, ND: Energy & Environmental Research Center, 2003.
[2] L. Heebink, et al., A Review of Literature Related to the Use of Spray Dryer Absorber Material: Production, Characterization, Utilization Applications, Barriers, and Recommendations, Draft Final Report Prepared for EPRI, Unpublished work, 2006.
[3] J.L. Getler, H.L. Shelton, D.A. Furlong, Modeling the spray absorption process for S02 removal, J. Air Pollut. Control Assoc. 29 (12) (1979) 1270–1274.
[4] ACAA, Coal Combustion Product Production and Use Survey. 2016: Aurora, CO.
[5] B. Jewell, et al. Spray Dryer Absorber Material: Cementitious Applications. in World of Coal Ash. 2017.
[6] P.-C. Aitcin, Cements of yesterday and today: concrete of tomorrow, Cem. Concr. Res. 30 (9) (2000) 1349–1359.
[7] L.K. Turner, F.G. Collins, Carbon dioxide equivalent (CO2-e) emissions: a comparison between geopolymer and OPC cement concrete, Constr. Build. Mater. 43 (2013) 125–130.
[8] M. De Andrade Cruz et al., Impact of solid waste treatment from spray dryer absorber on the levelized cost of energy of a coal-fired power plant, J. Clean. Prod. 164 (2017) 1623–1634.
[9] P.S.B. Bloem, Applications of spray-dry products in building materials, Proceedings of the Second International Conference on FGD and Chemical Gypsum, 1991. Toronto, Canada.
[10] R. Ailing et al., Effects of calcium sulfite on retarding of cement, 2009 3rd International Conference on Bioinformatics and Biomedical Engineering, IEEE, 2009.
[11] K. Redinger, Spray Dryer Atomization (SDA) byproducts: production, characteristics, and management options, In Proceedings of the 20th Symposium on Western Fuels, 2006. Denver, CO.
[12] R. Jewell, T. Robl, K. Ladwig, Use of Spray Dryer Absorber Material as a Replacement for Portland Cement in Concrete, Electric Power Research Institute, 2015, p. 164.
[13] J.M. Bigham et al., Mineralogical and engineering characteristics of dry flue gas desulfurization products, Fuel 84 (14–15) (2005) 1839–1848.
[14] H. Lee, V. Vimonsatit, P. Chindaprasirt, Residual strength of blended cement pastes and mortar exposed to elevated temperatures, Electron. J. Struct. Eng. 16 (1) (2016) 26–37.
[15] I. Demir et al., Examination of microstructure of fly ash in cement mortar, Int. J. Adv. Mech. Civ. Eng. 5 (1) (2018) 49–51.
[16] J. Stark, K. Bollmann, Delayed Ettringite Formation in Concrete, Nordic Concrete Research-Publications, 2000, pp. 4–28.
[17] S. Goni, A. Guerrero, SEM/EDX characterization of the hydration products of belite cements from class C coal fly ash, J. Am. Ceram. Soc. 90 (12) (2007) 3915–3922.
[18] H. Cornelissen, Spray dry absorption residue in concrete products, in: Studies in Environmental Science, Elsevier, 1991, pp. 499–506.
[19] K.G. Jeppesen, The effect on cement mortar and concrete by admixture of spray drying absorption products, MRS Online Proc. Lib. Arch. (1989) 178.
[20] A.R. Chini, L.C. Muszynski, J.K. Hicks. Determination of acceptance permeability characteristics for performance-related specifications for Portland cement concrete. 2003.
[21] T. Rupnow, P. Icenogle, Surface resistivity measurements evaluated as alternative to rapid chloride permeability test for quality assurance and acceptance, Transp. Res. Rec. 2290 (2012) 30–37.
[22] P. Ghosh, Q. Tran, Correlation between bulk and surface resistivity of concrete, Int. J. Concr. Struct. Mater. 9 (1) (2015) 119–132.
[23] I. Soroka, N. Stern, Calcareous fillers and the compressive strength of Portland cement, Cem. Concr. Res. 6 (3) (1976) 367–376.
[24] T. Sebök, J. Šimoník, K. Kulísek, The compressive strength of samples containing fly ash with high content of calcium sulfate and calcium oxide, Cem. Concr. Res. 31 (7) (2001) 1101–1107.
[25] V. Malhotra, Durability of concrete incorporating high-volume of low-calcium (ASTM Class F) fly ash, Cem. Concr. Compos. 12 (4) (1990) 271–277.